Luminescent Polymer Containing the Eu(III) Complex Having Fast Radiation Rate and High Emission Quantum Efficiency

Yasuchika Hasegawa,[†] Masaki Yamamuro,[†] Yuji Wada,[†] Nobuko Kanehisa,[‡] Yasushi Kai,[‡] and Shozo Yanagida*[,†]

Material and Life Science, Graduate School of Engineering, Osaka University, 2-1 Yamadaoka Suita, Osaka 565-0871, Japan, and Department of Materials Chemistry, Graduate School of Engineering, Osaka University, 2−1 Yamadaoka Suita, Osaka 565-0871, Japan

Received: November 8, 2002

Radiation rates and emission quantum yields of Eu(III) were modified using asymmetric deuterated Eu(III) complexes doped in poly(methyl methacrylate) (PMMA) deuterated tris-(hexafluoroacetylacetonato)europium-(III) with phospine oxide in order to produce lowthreshold levels for laser transmission and amplifier emissions. Geometric structures of asymmetric Eu(III) complexes were determined by single-crystal X-ray diffraction and Judd−Ofelt analysis. Luminescent polymers were fabricated by incorporating Eu(III) complexes in a PMMA matrix. Luminescent PMMA containing Eu(hfa-D)$_3$(DPFBPO)$_2$ exhibited the highest quantum yield and fastest radiation rate (quantum yield = 78 ± 6%, radiation rate =1.2 × 10^3 s^{-1}) of the PMMA matrixes. Emission quantum yields of Eu(hfa-D)$_3$ (TPPO)$_2$ in acetone-d_6 were found to be >95%. This radiation rate is of the same order as values reported for Nd:YAG. Prepared luminescent polymers including Eu(hfa-D)$_3$-(TPPO−F)$_2$ showed promising results for applications to novel organic Eu(III) devices, such as organic liquid lasers, plastic lasers, and optical fibers.

Introduction

Europium(III) complexes have been regarded as attractive for use as luminescent materials because of their red emissions (615 nm).[1] Characteristic emissions of Eu(III) complexes mainly come from electric dipole transitions.[2] Transition from the 4f inner shell of free Eu(III) is forbidden because it does not correlate with the change of parity. However, transitions that are forbidden by odd parity become partially allowed by mixing 4f and 5d states through ligand field effects of designed Eu(III) complexes.[3] An important purpose of the studies described here is to determine how electron transitions in Eu(III) can be manipulated by molecular design of Eu(III) complexes. Because red emissions from Eu(III) complexes are attributed to level 4 transitions, population inversion in 4f orbitals is a great advantage in the development of organic chelate laser and plastic optical fiber applications.[2,4] We have designed a Eu(III) complex with higher emission quantum yields and faster radiation rates than conventional Eu(III) complexes.

Eu(III) complexes that exhibit both high emission quantum yields and fast radiation rates are desirable luminescent materials for laser and fiber applications. Thus, Eu(III) complexes are designed to meet two criteria: (1) higher emission quantum yields to increase ρ_s (energy density) values and (2) faster radiation rates to produce large B (Einstein coefficient) values (see Appendix A).

To increase emission quantum yields, it is first necessary to suppress radiationless transitions caused by vibrational excitations. According to energy gap theory,[5] such radiationless transitions are promoted by ligands and solvents with high-frequency vibrational modes. In earlier studies, we reported the suppression of radiationless quenching in fluid Nd(III) systems by complexing Nd(III) with β-diketonato ligands composed only of low vibrational C−D and C−F bonds.[6a] Suppression of such vibrational excitations in Eu(III) complexes requires deuteration of C−H and O−H bonds or replacement of C−H bonds with C−F bonds in ligating molecules. Second, geometric structures of Eu(III) complexes should be 8 coordinate (square anti prism structure) in order to achieve stronger electric dipole radiation. Square anti prism structured Eu(III) complexes are expected to have increased radiation rates and quantum yields because of increases in $^5D_0 \rightarrow {}^7F_2$ emissions (electronic dipole transition), related to odd parity. Phosphine oxide ligands can produce antisymmetrical structures that promote faster radiation rates. Furthermore, increased emission quantum yields of Eu(hfa-D)$_3$-(phosphine oxide)$_2$ can be expected, because coordination of phosphine oxide molecules (1) prevents coordination of water or solvent molecules and (2) lowers vibrations (P = O:1125 cm^{-1}).

Here, we report studies into deuterated Eu(III) complexes with fast radiation rates and high luminescence quantum efficiencies and fabrication of effective luminescent organic polymers by incorporating luminescent Eu(III) complexes into poly(methyl methacrylate) (PMMA) matrixes. The complexes were deuterated tris(hexafluoroacetylacetonato)europium(III) with phospine oxide (complex **1**, Eu(hfa-D)$_3$(DPFBPO)$_2$; complex **2**, Eu(hfa-D)$_3$(TPPO)$_2$; complex **4**, Eu(hfa-D)$_3$(TPPO)$_2$(DMSO-d_6)$_n$), as shown in Figure 1, which were designed using findings from research into Nd(III) complexes. Suppression of vibrational excitations using complexes **1**, **2**, and **4** was more pronounced than that reported for Eu(TTA)$_3$(phospine oxide)$_2$ because of lower vibrational hfa-D ligands.[7] We discuss characteristics of Eu(III) complexes and luminescent polymers in terms of emission properties, Judd−Ofelt analysis, and X-ray fine structure analysis. We have successfully developed luminescent

* To whom correspondence should be addressed.
[†] Material and Life Science, Osaka University.
[‡] Department of Materials Chemistry, Osaka University.

10.1021/jp022397u CCC: $25.00
Published on Web 02/25/2003

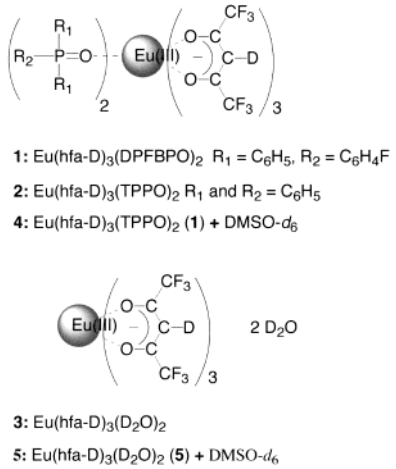

Figure 1. Chemical structure of samples **1**, **2**, **3**, **4**, and **5**.

PMMA using complex **1**, which exhibited the highest quantum yield and fastest radiation rate (quantum yield = 78 ± 6%, radiation rate $=1.2 \times 10^3\ s^{-1}$) of PMMA materials (>95% in acetone-d_6). Radiation rates of complex **2** in PMMA are of the same order as those of Nd:YAG, etc. (radiation rate $\approx 1.5 \times 10^3\ s^{-1}$). Luminescent PMMA appears to be the most suitable material for plastic laser or optical fiber applications. Conceptual design of Eu(III) complexes and fabrication of luminescent polymers is expected to open up pioneering fields in material science.

Experimental Section

Apparatus. Infrared spectra used to identify synthesized materials were obtained with a Perkin-Elmer FT-IR 2000 spectrometer. Elemental analyses were performed with a Perkin-Elmer 240C. ^{13}C and ^{19}F NMR data were obtained with a JEOL EX-270 spectrometer. ^{13}C NMR chemical shifts were determined using tetramethylsilane (TMS) as an internal standard, whereas ^{19}F NMR chemical shifts were determined using hexafluorobenzene as an external standard ($\delta = -162.0$ (s, Ar−F) ppm).

Materials. Europium acetate monohydrate (99.9%), 1,1,1,5,5,5-hexafluoro-2,4-pentanedione (hfa-H_2), and triphenylphosphine oxide (TPPO) were purchased from Wako Pure Chemical Industries Ltd. Methanol-d_4 (CD_3OD, 99.8%) and DMSO-d_6 (CD_3SOCD_3, 99.8%) were obtained from Aldrich Chemical Co. Inc. All other chemicals were reagent grade and were used as received.

Preparation of tris(Hexafluoroacetylacetonato)europium-(III) Dehydrates (Eu(hfa-H)$_3$(H$_2$O)$_2$). Europium acetate monohydrate (5.0 g, 12.5 mmol) was dissolved in 20 mL of distilled water by stirring at 0 °C. A solution of 1,1,1,5,5,5-hexafluoro-2,4-pentanedione (7 g, 33.6 mmol) in methanol (5 mL) was added dropwise to the above solution. The mixture produced a precipitation of white yellow powder after stirring for 3 h. The reaction mixture was filtered. The resulting white yellow needle crystals were recrystallized in methanol/water. Yield: 95%. IR-(KBr): 1650 (st, C═O), 1258−1145 (st, C−F) cm^{-1}. ^{19}F NMR (CD_3COCD_3) $\delta = -72.80$ (s, CF_3) ppm. Anal. Calcd for $C_{15}H_7O_8F_{18}Eu$: C, 22.48; H, 0.88%. Found: C, 22.12; H, 1.01%. Decomposition point: 220 °C (dehydration point: °C).

Preparation of tris(Hexafluoroacetylacetonato)europium-(III) bis(triphenylphospine oxide) (Eu(hfa-H)$_3$(TPPO)$_2$). Methanol (100 mL) containing Eu(hfa-H)$_3$(H_2O)$_2$ (4.28 g, 6 mmol) and triphenylphospine oxide (TPPO) (2.78 g, 10 mmol) was refluxed under stirring for 12 h. The reaction mixture was concentrated using a rotary evaporator. Reprecipitation by addition of excess hexane solution produced crude crystals, which were washed in toluene several times. Recrystallization from hot toluene/cyclohexane gave white needle crystals ([Eu-(hfa-H)$_3$]·2(TPPO)). Yield: 74%. IR(KBr): 1650 (st, C═O), 1250−1150 (st, C−F), 1125 (st, P═O) cm^{-1}. ^1H NMR (CD_3-$COCD_3$) $\delta = 7.6$ (m, aromatic C−H), 5.4 (s, c−H) ppm. ^{19}F NMR (CD_3COCD_3) δ=-76.7 (s, C−F) ppm. Anal. Calcd for $EuC_{51}H_{33}O_8F_{18}P_2$: C, 45.96; H, 2.50%. Found: C, 45.94; H, 2.57%. Decomposition point: 250 °C.

Preparation of Diphenyl-p-fluorobenzene-phosphine oxide (DPFBPO). DPFBPO was obtained using the same method as previously reported.[8] White crystals. Yield: 30%. ^1H NMR (CD_3COCD_3) $\delta = 7.29-7.37$ (m, aromatic C−H, 1H), 7.51−7.82 (m, aromatic C−H, 6H) ppm. ^{19}F NMR (CD_3COCD_3) $\delta = -106.37$ (s, aromatic C−F) ppm. Anal. Calcd for $C_{18}H_{14}$-$O_1F_1P_1$: C, 72.97; H, 4.76%. Found: C, 72.79; H, 4.87%. EIS-MS=297.0 ((TPPO−F)H^+).

Preparation of tris(Hexafluoroacetylacetonato)europium-(III) bis(tri-*n*-butylphosphine oxide) (Eu(hfa-H)$_3$(DPFBPO)$_2$). Eu(hfa-H)$_3$(DPFBPO)$_2$ was obtained by the reaction of Eu(hfa-H)$_3$(H_2O)$_2$ with TPPO−F in methanol at 70 °C for 12 h. Recrystallization from hot toluene/cyclohexane gave white needle crystals (Eu(hfa-H)$_3$(TPPO−F)$_2$). Yield: 53%. IR-(KBr): 1650 (st, C═O), 1260−1150(st, C−F), 1150−1100 (st, P═O) cm^{-1}. ^1H NMR (CD_3COCD_3) $\delta = 7.6$ (m, aromatic C−H), 5.4 (s, c−H) ppm. ^{19}F NMR (CD_3COCD_3) $\delta = -76.7$ (s, C−F), $\delta = -106.37$ (s, aromatic C−F) ppm. Anal. Calcd for $EuC_{51}H_{33}O_8F_{18}P_2$: C, 69.06; H, 5.07%. Found: C, 68.42; H, 5.16%. EIS-MS = 1159.6 (Eu(hfa-H)$_2^+$(TPPO−F)$_2$).

Crystallography. Colorless single crystals of complex **2** were mounted on a glass fiber using epoxy resin. X-ray diffraction intensities were collected with a Rigaku AFC-5R four-circle diffractometer using graphite-monochromated Mo Kα radiation in $\omega-2\theta$ scan mode. Corrections for decay and Lorentz-polarization effects were made, with empirical absorption corrections solved by direct methods[9] and expanded using Fourier techniques.[10] Non-hydrogen atoms were refined anisotropically. Hydrogen atoms were placed in calculated positions (C−H 0.95 Å) but not refined. The final cycle of full-matrix least-squares refinement was based on observed reflections and variable parameters. All calculations were performed using the TEXSAN crystallographic software package.

Preparation of Deuterated Eu(III) Complexes. Eu(III) complexes (0.1 mmol) were dissolved in 2 mL of CD_3OD. After degassing the solution, deuteration was carried out by exchange reactions via keto−enol tautomerism in CD_3OD for 6 h under vacuum. After evaporation under vacuum ($\sim 10^{-3}$ Torr), deuterated Eu(III) complexes, Eu(hfa-D)$_3$(DPFBPO)$_2$, Eu(hfa-D)$_3$-(TPPO)$_2$, and Eu(hfa-D)$_3$(D_2O)$_2$, were obtained as white yellow powders.

Preparation of Polymethylmethacryrate (PMMA) Containing Eu(III) Complexes. Deuterated Eu(III) complex (0.05 M) was dissolved in a 1-mL mixture of purified anhydrous methyl methacrylate (MMA) and AIBN in a Pyrex tube (Eu(III) ion 0.7w%, AIBN 0.05w%, and DMSO-*d*6 6.6w%). The Pyrex tube was sealed off under 10^{-3} Torr and thermostated at 60 °C for polymerization of MMA (samples **1**, **2**, and **4**). For comparison, PMMA polymers incorporating DMSO-d_6 and Eu(hfa-D)$_3$(D_2O)$_2$ or Eu(hfa-D)$_3$(TPPO)$_2$ were similarly prepared (samples **3** and **5**). After polymerization, optical samples were ground using Al_2O_3 nanoparticles.

Optical Measurements. Emission spectra were measured at room temperature using a HITACHI F-4500 system. The spectra

TABLE 1: Selected Bond Length (Å) for Complex 2

bond	length/Å	bond	length/Å	bond	length/Å	bond	length/Å
Eu1−O1	2.41	O7−P1	1.49	C16−C17	1.38	C34−C35	1.38
Eu1−O2	2.39	O8−P2	1.48	C17−C18	1.39	C35−C36	1.38
Eu1−O3	2.44			C18−C19	1.39	C36−C37	1.36
Eu1−O4	2.42	P1−C16	1.81	C19−C20	1.35	C37−C38	1.38
Eu1−O5	2.41	P1−C22	1.79	C20−C21	1.39	C38−C39	1.38
Eu1−O6	2.41	P1−C28	1.78	C21−C16	1.38	C39−C34	1.36
		P2−C34	1.81	C22−C23	1.37	C40−C41	1.37
Eu1−O7	2.32	P2−C40	1.78	C23−C24	1.39	C41−C42	1.38
Eu1−O8	2.31	P2−C46	1.79	C24−C25	1.34	C42−C43	1.34
				C25−C26	1.34	C43−C44	1.35
O1−C1	1.25	C1−C2	1.38	C26−C27	1.38	C44−C45	1.35
O2−C3	1.26	C2−C3	1.37	C27−C22	1.38	C45−C40	1.38
O3−C6	1.24	C6−C7	1.39	C28−C29	1.38	C46−C47	1.40
O4−C8	1.25	C7−C8	1.36	C29−C30	1.37	C47−C48	1.38
O5−C11	1.24	C11−C12	1.38	C30−C31	1.33	C48−C49	1.37
O6−C13	1.24	C12-c13	1.38	C31−C32	1.35	C49−C50	1.41
				C32−C33	1.38	C50−C51	1.41
				C33−C28	1.37	C51−C46	1.37
average of Eu−O1∼6	2.41	average of O−P	1.48	average of C−C	1.36	average of C−C	1.38
average of Eu−O7∼8	2.31	average of P−C	1.79				

were corrected for detector sensitivity and lamp intensity variations. Emission lifetimes were measured with a Q switched Nd:YAG laser (Spectra Physics, INDI-50, fwhm = 5 ns, λ = 1064 nm) and photomultiplier (Hamamatsu photonics, R7400U-03, response time ≤ 0.78 ns). Nanosecond light pulses used to produce excitations in the samples (λ = 465 nm, power = 0.1 mJ) were generated by a dye laser (USHO optical systems DL-50, dye = coumarin 120). Emissions from the samples were filtered using a monochromator (Shimazu SPG-100ST) placed in front of the detector. Nd:YAG response was monitored with a digital oscilloscope (Sony Tektronix, TDS3052, 500 MHz) synchronized to the single pulse excitation.

Quantum yields were determined using a standard integrating sphere (diameter 6 cm).[11] Optical path length of the cell was 5 mm. Corrected intensity functions of the excitation ($I_{ex}(\lambda_{ref})$: without sample) were determined by the excitation spectra of the system ($g_{ref}(\lambda)$: without a sample, 450 nm − 480 nm, scan rate = 60 nm/min)

$$I_{ex}(\lambda_{ref}) = \frac{\phi}{\int g_{ref}(\lambda)\, d\lambda} g_{ref}(\lambda) \quad (1)$$

In eqs 1 and 2, ϕ is light intensities of excitation. Corrected intensity functions of light absorption with sample, $I_{ex}(\lambda_{sam})$, were also determined from excitation spectra of the system (450 nm − 480 nm, scan rate = 60 nm/min), whereas the corrected intensity function of the emission was determined from emission spectra ($I_{em}(\lambda)$, 550 nm − 800 nm, scan rate = 60 nm/min). Quantum yield, Φ, was calculated from

$$\Phi = \frac{N_{emission}}{N_{absorption}} = \frac{\int \frac{\lambda}{hc} I_{em}(\lambda)\, d\lambda}{\int \frac{\lambda}{hc}\{I_{ex}(\lambda_{ref}) - I_{ex}(\lambda_{sam})\}\, d\lambda} \quad (2)$$

Quantum yields of OPP-3 (Ex at 285 nm, 300−450 nm, emission quantum yield = 95 ± 5%) and Rhodamine 6G in PMMA (Ex at 488 nm, 510−760 nm, emission quantum yield = 93 ± 3%) determined by the present procedure agreed well with reported values.[12]

Judd−Ofelt Analysis. Absorption spectra of $Eu(NO_3)_3$ and Eu(III) complexes were measured at room temperature using a HITACHI U-3300 system. Judd−Ofelt analysis of $Eu(NO_3)_3$ in DMSO-*d*6 was carried out using $^7F_0 \rightarrow {}^5D_{1-3}$ and $^7F_0 \rightarrow {}^5L_6$ transitions. The Eu(III) complexes exhibited broad absorption peaks due to $\pi-\pi^*$ transitions in the ligands. Judd−Ofelt analysis of Eu(III) complexes was carried out using the $^7F_0 \rightarrow {}^5D_2$ transition (465 nm). Concentration of the Eu(III) complexes in solvent was 0.05 M. Details of the analysis are described in Appendix B.

Semiempirical MO Calculations. Calculations of the charge distributions of DMSO and TPPO molecules were carried out by MOPAC ver.6.10 (MM2/PM3) using the CAChe system.

Results

Geometrical Structure. The crystal structure of sample **2** was determined by single-crystal X-ray diffraction. Selected bond lengths are listed in Table 1. Sample **2** contained an asymmetric structure with TPPO molecules as shown in Figure 2a. The two Eu−O bonds with TPPO ligands (2.32 and 2.31 Å) were shorter than the six Eu−O bonds with hfa ligands (2.39−2.44 Å). From coordination site angles, the geometrical structure was determined to be an antisymmetrical square-anti prism (Figure 2b). This result indicates that sample **2** has no inverted center in the crystal field, resulting in an increase in electron transitions in the 4f orbitals due to odd parity. Crystal structures of TPPO ligands in sample **2** were compared to those of TPPO molecules.[13] Average bond lengths of P−O, P−C, and C−C in sample **2** were found to be 1.48, 1.79, and 1.37 Å respectively, slightly shorter than those of TPPO molecules (1.49, 1.80, and 1.39 Å). TPPO ligands in sample **2** would also be affected by the coordination of Eu(III).

Emission Properties in Polymer. To examine photophysical properties of Eu(III) ions with various ligands in PMMA, emission spectra and emission lifetimes were measured for the excitation at 465 nm ($^7F_0 \rightarrow {}^5D_2$: f−f transition). Emission spectra of Eu(III) complexes in PMMA are shown in Figure 3a. Emission bands were observed at 578, 590, 613, 651, and 698 nm and are attributed to f−f transitions $^5D_0 \rightarrow {}^7F_0$ (zero-zero band: forbidden transition), $^5D_0 \rightarrow {}^7F_1$ (magnetic dipole transition), $^5D_0 \rightarrow {}^7F_2$, $^5D_0 \rightarrow {}^7F_3$, and $^5D_0 \rightarrow {}^7F_4$ (electronic dipole transitions), respectively. Spectra shown in Figure 3a were normalized with respect to the $^5D_0 \rightarrow {}^7F_1$ (magnetic dipole) transition. $^5D_0 \rightarrow {}^7F_2$ transition intensities of samples **1** and **2** were found to be the largest of the complexes used in our experiments. Emission decays of Eu(III) complexes in PMMA were also measured (Figure 3b,c). Single-exponential decay emissions indicated the presence of a single luminescent site in

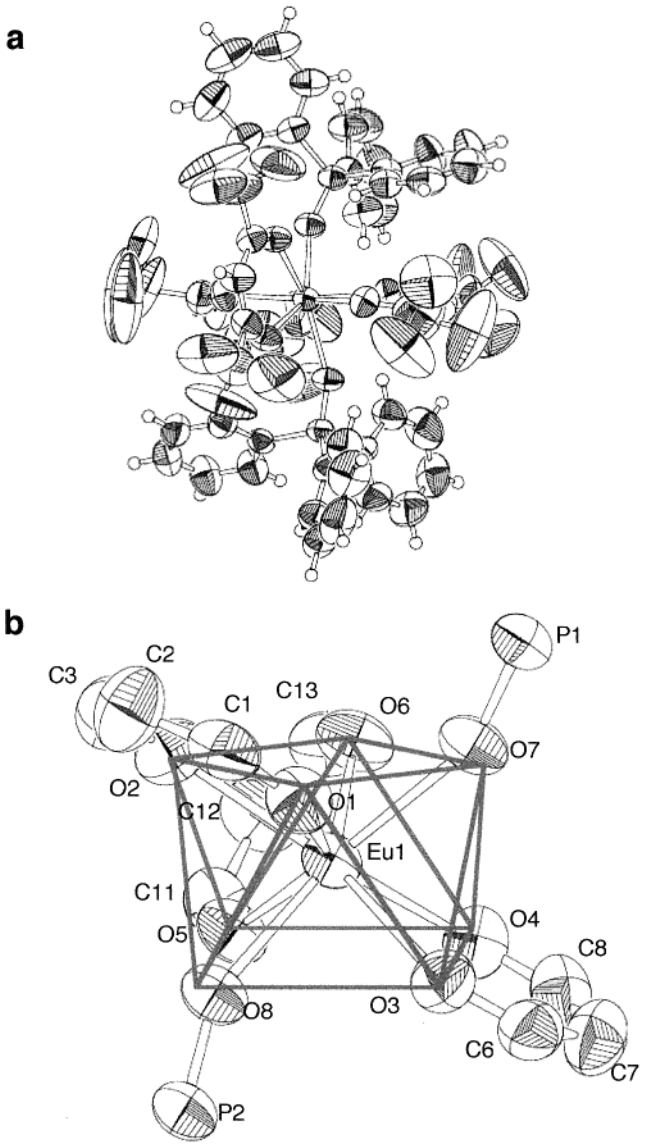

Figure 2. (a) ORTEP view of sample **2**. (b) ORTEP view of samples **2** coordination sites.

PMMA and homogeneity of the samples. Emission lifetimes were determined from the slopes of logarithmic plots of decay profiles. Emission lifetimes, quantum yields, and calculated emission rates are summarized in Table 4. Luminescent polymer **1** exhibited the highest quantum yield (78 ± 6%) and fastest emission rate (1.2×10^3 s^{-1}) in PMMA matrix. $^5D_0 \rightarrow {}^7F_2$ transition intensities of Eu(III) complexes with DMSO-d_6 (samples **4** and **5**) were smaller than those of the corresponding complexes without DMSO-d_6 (samples **1**, **2**, and **3**). The emission quantum yield of sample **2** in acetone-*d*6 was found to be >95%, whereas the quantum yield was calculated to be 99.2% using Judd−Ofelt analysis.

Discussion

Molecular Design. The creation of lanthanide(III) complexes with higher emission quantum yields is directly linked to suppression of radiationless transitions caused by vibrational excitations in surrounding media.[6] In contrast, radiation rates of Eu(III) complexes are linked to geometric structure. If there is no inversion symmetry at lanthanide ion sites, uneven ligand field components can mix with opposite-parity states in $4f^n$-configuration levels. Electric-dipole transitions are then no longer strictly forbidden in the ligand fields, resulting in faster electron transition radiation rates.[2] Eu(III) complexes with odd parity can be created using certain geometrical and coordination structures.

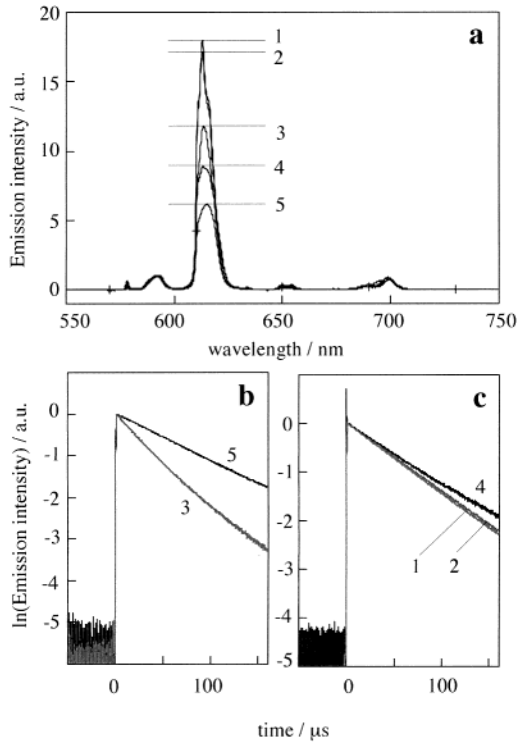

Figure 3. (a) Emission spectra of samples **1**, **2**, **3**, **4**, **5**, and **6** in PMMA (Eu: 0.7 w%). The excitation at 465 nm is due to the $^7F_0 \rightarrow {}^5D_2$ transition. Spectra in Figure 3a were normalized with respect to the $^5D_0 \rightarrow {}^7F_1$ (magnetic dipole) transition. (b and c) Emission decays profile of samples **1**, **2**, **3**, **4**, **5**, and **6** in PMMA (Eu: 0.7 w%) shown on a logarithmic scale. Excitation at 465 nm ($^7F_0 \rightarrow {}^5D_2$) was caused by a dye laser (coumarin 120).

TABLE 2: Crystal Data, Data Collection, and Structure Refinement for Complex 2

	complex **2**
chemical formula	$EuC_{51}H_{33}O_8F_{18}P_2$
formula weight	1329.71
crystal system	monoclinic
space group	$P2_1/c$ (no. 14)
a/Å	13.3(1)
b/Å	13,5(1)
c/Å	30.5(1)
β/°	90.4(5)
V/Å^3	5475(59)
Z	4
T/°C	23.0
μ(Mo Kα)/cm^{-1}	13.13
no. of measured reflections	13921
no. of unique reflections	12666
R_{int}	0.019
$R(R_w)$	0.057 (0.062)

TABLE 3: Judd−Ofelt Parameters of Eu(III) Complexes in Organic Solvents

run	complex	matrix	Judd-Ofelt parameter Ω2/ 10^{-20} cm^2
1	$Eu(hfa)_3(DPFBPO)_2$	acetone	27
2	$Eu(hfa)_3(TPPO)_2$	acetone	26
3	$Eu(hfa)_3(H_2O)$	acetone	15
4	$Eu(hfa)_3(TPPO)_2$	DMSO	14
5	$Eu(hfa)_3(H_2O)_2$	DMSO	13
6	$Eu(NO_3)_3$	DMSO	1

TABLE 4: Emission Quantum Yields, Emission Lifetimes, and Radiation Rates of Eu(III) Complexes in Polymer Matrixes[a]

run	complex	matrix[b]	emission quantum yield/%	emission lifetime/ms	radiation rate/$\times 10^2 s^{-1}$
1	Eu(hfa-D)$_3$(DPFBPO)$_2$	PMMA	78 ± 6	0.67 ± 0.005	12
2	Eu(hfa-D)$_3$(TPPO)$_2$	PMMA	75 ± 5	0.71 ± 0.005	11
3	Eu(hfa-D)$_3$(D_2O)$_2$	PMMA	23 ± 5	0.41 ± 0.005	5.6
4	Eu(hfa-D)$_3$(TPPO)$_2$(DMSO-d_6)$_n$[c]	PMMA	65 ± 11	0.75 ± 0.005	8.6
5	Eu(hfa-D)$_3$(DMSO-d_6)$_n$[c]	PMMA	46 ± 3	0.86 ± 0.005	5.3
6	Eu(hfa-D)$_3$(TPPO)$_2$	acetone-d_6	>95	0.94 ± 0.005	

[a] The emission quantum yields and lifetimes of the Eu(III) complexes were measured by the excitation at 465 nm ($^7F_0 \rightarrow {}^5D_2$). Radiation rate = emission quantum yield/emission lifetime. [b] Composition of polymerization; Eu(III), 0.7 w%; AIBN, 0.05 w%. [c] Composistion of DMSO-d_6; 6.6 w%.

Coordination numbers of lanthanide ions in solution are known to vary between 8 and 10 depending on the nature of the ligating molecules.[14] Generally, the Ln(hfa-D)$_3$ complex has two coordinating water or solvent molecules in solution.[6,15] The 8 coordinate Eu(III) complex was synthesized using [Eu(hfa-D)$_3$] and two phosphine oxide molecules. MOPAC charges of O atoms in TPPO (triphenylphosphine oxide) are found to be -0.80 by MO calculations. This indicates that the coordination ability of phosphine oxide is stronger than that of DMSO, methanol, acetone, or H_2O.[6d] Furthermore, structural analysis by single-crystal X-ray diffraction indicates that Eu(III) samples **1** and **2** maintain 8 coordinate (anti-square prism) structures, resulting in faster radiation rates. Samples **1** and **2** have more allowed transitions than tris-β-diketonato Eu(III) complexes such as sample **3** because of odd parity.

Judd−Ofelt Analysis. Judd−Ofelt analysis is a useful tool for estimating the population of odd parity electron transitions.[17] Interaction parameters of ligand fields are given by the Judd−Ofelt parameters, Ω_λ. In particular, Ω_2 is more sensitive to the symmetry and sequence of ligand fields. To produce faster Eu(III) radiation rates, anti-symmetrical Eu(III) complexes with larger Ω_2 parameters need to be designed. Ω_2 parameters of Judd−Ofelt analyses are shown in Table 3. Ω_2 values of Eu(hfa-D)$_3$(phosphine oxide)$_2$ (samples **1** and **2**) in acetone were found to be 27×10^{-20} cm^2 and 26×10^{-20} cm^2 respectively. These values were larger than that of sample **3** Eu(hfa-D)$_3$(D_2O)$_2$, 15×10^{-20} cm^2. Comparison of Ω_2 parameters indicates that electron transition probabilites in samples **1** and **2** are much larger than those of sample **3**, in agreement with the faster emission rates observed, as shown in Table 4. In contrast, Ω_2 values of Eu(III) complexes in DMSO (**4**, 14×10^{-20} cm^2 and **5**, 13×10^{-20} cm^2) were smaller than those in acetone. We propose that coordination of DMSO molecules to Eu(III) ions leads to a decrease in Ω_2 and thus in the probability of electronic dipole transitions.

Geometrical Structure and Emission Properties in PMMA. Emission strengths of samples **1**, **2**, **3**, **4**, and **5** in PMMA are in order of the degree of odd parity, in agreement with predictions of Judd−Ofelt analysis. Comparison of emission intensities demonstrates the importance of using asymmetrical molecules in luminescent materials. $^5D_0 \rightarrow {}^7F_2$ transition intensities and emission rates of Eu(III) complexes with DMSO-d_6 (samples **4** and **5**) were smaller than those of complexes without DMSO-d_6 (samples **1**, **2**, and **3**), indicating that the presence of DMSO-d_6 molecules leads to a decrease in the odd-parity of Eu(III) complexes.

Previously, we reported the highest emission quantum yields of lanthanide(III) in DMSO-d_6 and polymer matrixes by the formation of 12-coordinate lanthanide(III) complex consisting of three HFA-D ligands and six DMSO-d_6 molecules.[6a,11] Deuterated DMSO molecules, which have a lower vibrational structure (S═O, 1355 cm^{-1}) and the strongest coordination ability of the examined solvents, replace D_2O molecules in the vicinity of Nd(HFA-D)$_3$, preventing radiationless transitions to D_2O. However, formation of symmetrical 12-coordinate lanthanide(III) complex containing DMSO-d_6 molecules leads to weaker electric dipole radiation, so that optical transmissions are dominated by magnetic dipole transitions, which are forbidden by odd parity, resulting in a lower emission rate.[6a] Lower electron transition rates in Eu(III) complexes with DMSO-d_6 (samples **4** and **5**) are due to the formation of more symmetrical structures, such as 12 coordinated.

The comparison of sample **2** with **6** is explained as being due to radiationless transition via vibrational excitation of C−H bonds in the matrixes. The matrix effect for suppression of vibrational exciation was investigated by using Eu(hfa-D)$_3$-(DMSO-d_6)$_n$.[11] Emission efficiency of lanthanide(III) luminescent materials is depend on the percentage of H atoms. Weight percentage of H atoms in the resulting PMMA system was calculated to be 8.0%. To minimize the vibrational excitation of C−H bond in the matrix, we attempted to polymerize hexafluoroisopropyl methacrylate (FiPMA), i.e., C−F bond containing methacrylate, in the presence of Eu(HFA-D)$_3$ and DMSO-d_6. A transparent polyhexafluoroisopropyl methacrylate (P−FiPMA) polymer matrix was obtained by polymerization of FiPMA with 10% MMA. The system of Eu(HFA-D)$_3$-(DMSO-d_6) in P−FiPMA gave a quantum yield of 72 ± 7%, which was much larger than those in PMMA (quantum yield of 46%). The system of Eu(HFA-D)$_3$(DMSO-d_6) in P−FiPMA (the weight percentage of H atoms is 2.5%) was improved to give an effectively luminescent organic polymer of Eu(III). The vibrational harmonic bands of Eu(HFA-D)$_3$(DMSO-d_6)$_n$ in P−FiPMA was smaller than that in corresponding PMMA because of a smaller amount of H atoms. This result suggests that P−FiPMA matrix can suppress the radiationless transition via vibrational excitation.

Comparison of samples **1** and **2** shows a slight predominance of F atoms over H atoms in TPPO groups in terms of emission quantum yields and radiation rates. There is a correlation between emission analyses and Judd−Ofelt analyses of **1** and **2**. The low-vibrational environment and antisymmetric form of DPFBPO have an impact on electron transition rates. Luminescence properties of complex **1** demonstrate the importance of partial fluorination. Further design and synthesis of partially fluorinated ligands could lead to the creation of superlative luminescent materials.

Conclusion

Electron transitions of lanthanides can be manipulated by ligand design. In this paper, we introduced molecular design strategies for enhancing electron dipole transition rates. Quantum yields of luminescent materials using fluorine polymer with Eu(hfa-D)$_3$(DPFBPO)$_2$ are expected to be more than 90%.[11] Samples **1** and **2** do not affect the water, because the P═O ligand with the strongest coordination ability suppress the approach

of water in the coordination sites.[6d] The sample **2** has kept the same emission quantum yield (75%) for two years. Therefore, luminescent polymers including $Eu(hfa\text{-}D)_3(DPFBPO)_2$ are desirable for developing applications in novel organic Eu(III) devices, such as organic liquid lasers, plastic lasers and optical fibers.

Acknowledgment. We are grateful to Prof. R. Arakawa, Department of Applied Chemistry, Faculty of Engineering, Kansai University, for the EIS-MS measurements.

Appendix

A. Theory of Laser Transmission. A key goal in laser transmission and photoinduced amplification is to achieve smaller transmission threshold levels for practical uses. The transmission threshold, ΔN_{th}, can be expressed as

$$\Delta N_{th} = \frac{\Delta N_0}{1 + 2B\rho_s T} \tag{A1}$$

where ΔN_0, B, ρ_s, and T are the number of excited Eu(III) complexes (excited energy), Einstein coefficient, energy density, and relaxation time in cavity, respectively.[2] To obtain smaller ΔN_{th} values, Eu(III) complexes with larger B and $\rho_s$values need to be designed. Two criteria exist: (1) higher emission quantum yields to increase $\rho_s$values and (2) faster radiation rates to obtain large B values.

B. Judd−Ofelt Analysis. In Judd−Ofelt treatment, the oscillator strength between two states i and j in 4f orbitals is given by

$$f(i\rightarrow j)\frac{2J+1}{e^2 v} = \sum_{\lambda=2,4,6} \Omega_\lambda |\langle i|U^\lambda|j\rangle|^2 \tag{A2}$$

The left-hand side of the equation can then be expanded to

$$\frac{3h}{8\pi^2 cN}\frac{(n^2+2)^2}{9n}\int A\,d\lambda \frac{2J+1}{e^2\lambda_{max}\times 10^{-7}} = S_M \tag{A3}$$

where Ω_λ, U^λ, e, J, c, h, λ_{max}, N, η, and $\int A\,d\lambda$ are Judd-ofelt parameters (constants), tensor parameters, elementary charge (1.6022×10^{20} ems), angular momentum (Eu(III): 0), the speed of light (2.998×10^{-10} cm s^{-1}), Plank's constant (6.626×10^{-27} erg s), center wavelength at the absorption band (nm), density of ions in the matrix, refractive index of the solution, and absorption integral, respectively.[16] Tensor parameters U^λ of Eu(III) are given by[18]

$$U = \begin{bmatrix} {}^7F_0\rightarrow{}^5L_6 \\ {}^7F_0\rightarrow{}^5D_3 \\ {}^7F_0\rightarrow{}^5D_2 \\ {}^7F_0\rightarrow{}^5D_1 \end{bmatrix} U2 = \begin{bmatrix} 0.0000 \\ 0.0004 \\ 0.0008 \\ 0.0000 \end{bmatrix} U4 = \begin{bmatrix} 0.0000 \\ 0.0012 \\ 0.0000 \\ 0.0000 \end{bmatrix}$$

$$U6 = \begin{bmatrix} 0.0155 \\ 0.0000 \\ 0.0000 \\ 0.0000 \end{bmatrix} \tag{A4}$$

References and Notes

(1) Review on luminescence behaviors: Blasse, G.; Grabmaier, B. C. *Luminescent Materials*; Springer-Verlag, New York, 1994.

(2) Gan, F. *Laser Materials*; World Scientific: Singapore, 1995; p 70.

(3) Selected papers of luminescent Eu(III) complexes: (a) Charbonniere, L.; Ziessel R.; Guardigli, M.; Roda, A.; Sabbatini, N. *J. Am. Chem. Soc.* **2001**, *123*, 2436. (b) Yang, X.; Su, C.; Kang, B.; Feng, X.; Xiao, W.; Liu, H.; *J. Chem. Soc., Dalton Trans.* **2000**, *19*, 3253. (c) Son, H.; Roh, J.; Shin, S.; Park, J.; Ku, J. *J. Chem. Soc., Dalton Trans.* **2001**, *9*, 1524. (d) Bruce, J. I.; Dickins, R. S.; Govenlock L. J.; Gunnlaugsson, T.; Lopinski, S.; Lowe, M. P.; Parker, D.; Perry, J. J. B.; Aime, S.; Botta, M. *J. Am. Chem. Soc.* **2000**, *122*, 9674. (e) Fatin-Rouge, N.; Toth, E.; Perret, D.; Backer, R. H.; Merbach, A. E.; Buenzli, J. G. *J. Am. Chem. Soc.* **2000**, *122*, 10810. (f) Tsukube, H.; Hosokubo, M.; Wada, M.; Shinoda, S.; Tamiaki, H. *Inorg. Chem.* **2001**, *40*, 740. (g) Skinner, P. J.; Beeby, A.; Dickins, R. S.; Parker, D.; Aime, S.; Botta, M. *J. Chem. Soc., Perkin 2* **2000**, *7*, 1329. (h) Bunzli, J. G.; Charbonniere, L. J.; Ziessel, R. F. *J. Chem. Soc., Dalton Trans.* **2000**, 1917. (i) McGehee, M. D.; Bergstedt, T.; Zhang, C.; Saab, A. P.; O'Regan, M. B.; Bazan, G. C.; Srdanov, V. I.; Heeger, A. J. *Adv. Mater*. **1999**, *11*, 1349−1354. (j) Epstein, D. M.; Chappell, L. L.; Khalili, H.; Supkowski, R. M.; Horrocks, W. DeW., Jr.; Morrow, J. R. *Inorg. Chem.* **2000**, *39*, 2130. (k) Klink, S. I.; Grave, L.; Reinhoudt, D. N.; van Veggel, F. C. J. M.; Werts, M. H. V.; Geurts, F. A. J.; Hofstraat, J. W. *J. Phys. Chem. A* **2000**, *104*, 5457. (l) Lessmann, J. J.; Horrocks, W. DeW., Jr. *Inorg. Chem*. **2000**, *39*, 3114.

(4) (a) Schimitschek, E. J.; Schwarz, E. G. K. *Nature* **1962**, *196*, 832. (b) Samelson, H.; Brecher, C.; Brophy, V. *Appl. Phys. Lett* **1964**, *5*, 173. (c) Kobayashi, T.; Nakatsuka, S.; Iwafuji, T.; Kuriki, K.; Imai, N.; Nakamoto, N.; Claude, C. D.; Sasaki, K.; Koike, Y.; Okamoto, Y. *Appl. Phys. Lett.* **1997**, *71*, 2421−2423. (d) Kuriki, K.; Koike, Y.; Okamoto, Y. *Chem. Rev.* **2002**, *102*, 2347.

(5) Stain, G.; Würzberg, E. *J. Chem. Phys.* **1975**, *62*, 208.

(6) (a) Hasegawa, Y.; Iwamuro, M.; Murakoshi, K.; Wada, Y.; Arakawa, R.; Yamanaka, T.; Nakashima, N.; Yanagida, S. *Bull. Chem. Soc. Jpn.* **1998**, *71*, 2573. (b) Hasegawa, Y.; Ohkubo, T.; Sogabe, K.; Kawamura, Y.; Wada, Y.; Nakashima, N.; Yanagida, S. *Angew. Chem., Int. Ed*. **2000**, *39*, 357. (c) Wada, Y.; Okubo, T.; Ryo, M.; Nakazawa, T.; Hasegawa, Y.; Yanagida, S. *J. Am. Chem. Soc.* **2000**, *122*, 8583. (d) Hasegawa, Y.; Kimura, Y.; Murakoshi, K.; Wada, Y.; Kim, J.; Nakashima, N.; Yamanaka, T.; Yanagida, S. *J. Phys. Chem.* **1996**, *100*, 10201. (e) Hasegawa, Y.; Murakoshi, K.; Wada, Y.; Yanagida, S.; Kim, J.; Nakashima, N.; Yamanaka, T. *Chem. Phys. Lett.* **1996**, *248*, 8.

(7) Zhang, X.; Sun, R.; Zheng. Q.; Kobayashi, T.; Li, W. *Appl. Phys. Lett.* **1997**, *71*, 2596. $Eu(TTA)_3$(phospine oxide)$_2$ is well-known as a red luminescent complex for EL devises.

(8) Lin, Q.; Long, T. E. *J. Polym. Sci. Part A* **2000**, *38*, 3736.

(9) SIR 92; Altomare, A.; Burla, M. C.; Camalli, M.; Cascarano, M.; Giacovazzo, C.; Guagliardi, A.; Polidori, G. *J. Appl. Crystallogr.* **1994**, *27*, 435.

(10) DIRDIF 94; Beurskens, P. T.; Admiraal, G.; Bosman, W. P.; de Gelder, R.; Israel, R. and Smits, J. M. M. The DIRDIF 94 program system, Technical Report of the Crystallography Laboratory; University of Nijmegen: Nijmegen, The Netherlands, 1994.

(11) (a) Hasegawa, Y.; Sogabe, K.; Wada, Y.; Kitamura, T.; Nakashima, N.; Yanagida, S. *Chem. Lett*. **1999**, 35. (b) Hasegawa, Y.; Sogabe, K.; Wada, Y.; Yanagida, S. *J. Lumin*. In press.

(12) Lesiecki, M. L.; Drake, J. M. *Appl. Opt.* **1982**, *21*, 557.

(13) Brock, C.; Schweizer, W. B.; Dunitz, J. D. *J. Am. Chem. Soc.* **1985**, *24*, 6964.

(14) Recent reviews on lanthanide coordination chemistry: (a) Aime, S.; Botta, M.; Fasano, M.; Terreno, E. *Chem. Soc. Rev.* **1998**, *27*, 19. (b) Piquet, C.; Bünzli, J.-C. G. *Chem. Soc. Rev.* **1999**, *28*, 347. (c) Caravan, P.; Ellison, J. J.; McMurry, T. J.; Lauffer, R. B. *Chem. Rev.* **1999**, *99*, 2293.

(15) (a) Nakamura, M.; Nakamura, R.; Nagai, K.; Shimoi, M.; Tomoda, S.; Takeuchi, Y.; Ouchi, A. *Bull. Chem. Soc. Jpn*. **1986**, *59*, 332. (b) Hasegawa, Y.; Murakoshi, K.; Wada, Y.; Yanagida, S.; Kim, J.; Nakashima, N.; Yamanaka, T. *Chem. Phys. Lett*. **1996**, *248*, 8.

(16) (a) Capobianco, J. A.; Proulx, P. P. *Phys. Rev. B* **1990**, *42*, 5936. (b) Binnemans, K.; Van Deun, R.; Görller-Walrand, C.; Collinson, S. R.; Martin, F.; Bruce, D. W.; Wickleder, C. *Phys. Chem. Chem. Phys.* **2000**, *2*, 3753.

(17) Werts, M. H. V.; Jukes, R. T. F.; Verhoeven, J. W. *Phys. Chem. Chem. Phys.* **2002**, *4*, 1542.

(18) Carnall, W. T.; Fields, P. R.; Rajnak, K. *J. Chem. Phys.* **1968**, *49*, 4450.